Article

Hydrothermal Preparation of Faceted Vesicles Made of Span 40 and Tween 40 and Their Characterization

Toshinori Shimanouchi [1,*], Yui Komori [1], Kazuki Toramoto [1], Keita Hayashi [2], Kazuma Yasuhara [3], Ho-Sup Jung [4] and Yukitaka Kimura [1]

[1] Department of Environmental Chemistry and Materials, Okayama University, 3-1-1 Tsushima-naka, kita-ku, Okayama 700-8530, Japan

[2] National Institute of Technology, Nara College, 22 Yada-cho, Yamatokoriyama 630-8501, Japan

[3] Division of Materials Science, Nara Institute of Science and Technology (NAIST), 8916-5 Takayama-cho, Ikoma 630-8501, Japan

[4] Center for Food and Bioconvergence, Department of Food Science and Biotechnology, Seoul National University, Seoul 151-742, Republic of Korea

[*] Correspondence: tshima@cc.okayama-u.ac.jp

Abstract: The Span 40 (sorbitan monooleate)/Tween 40 (polyoxyethylene sorbitan monolaurate) system gives faceted vesicles with angular surfaces, rather than spherical vesicles. Herein, a continuous and facile preparation method, based on the subcritical water-assisted emulsification and solvent diffusion, was presented to yield faceted vesicles with two major and minor axes (Type A) and vesicles closer to a polyhedron (Type B). Type A, rather than Type B, vesicles were likely to be formed. From the measurements concerning ζ-potential, membrane fluidity, and the polarization environment of the membranes, faceted vesicles could be obtained at 0.25 wt% of the surfactant concentration. The phase-separated behavior of Span 40 and Tween 40 within vesicle membranes could explain the structural feature of faceted vesicles and calcein leakage behavior. The significant advantage is that Type A vesicles would be utilized as alternative drug carriers for others with low encapsulation efficiency, although the present technical limitations cause difficulty in the selective formation of Type A and B vesicles and the selection of adequate solvent to accelerate the solvent diffusion step.

Keywords: vesicles; subcritical water; emulsification; solvent diffusion

1. Introduction

A vesicle is a closed-system vesicle composed of a lipid bilayer membrane and is one of the molecular assemblies formed by lipids [1–6]. The particle size ranged from several tens of nanometers to several hundred micrometers. Amphiphilic molecules are known to form vesicles such as phospholipids (liposomes) [1–3], surfactants (niosomes) [4,5], and polymers (polymosomes) [6]. Since vesicles can encapsulate drugs in the internal aqueous phase and membrane, they are considered for various applications. For example, vesicles are vehicles that efficiently transport drugs into the body. Research is also underway for the application of detection assays based on the leakage characteristics of encapsulated substances, artificial cell systems, and new nanobioreactors. The search for and synthesis of lipid materials suitable for such applications is ongoing.

In recent years, some studies using Sorbitan Monooleate (Span)/Polyoxyethylene Sorbitan Monolaurate (Tween), which is cheaper than phospholipids, have shown progress [7–9]. The Spans have a sorbitol group as the hydrophilic head and an acyl chain in the hydrophobic tail. Tween is a molecule in which an oligoethylene glycol group is ether-bonded to the hydroxyl group at the head of the Span. The basic physical properties of the Span/Tween system are well known. However, unique features of vesicle formation have recently been discovered [8]. For example, Span 20/Tween 20 forms spherical vesicles (50:50), tubular

vesicles (100:0), and lens-like vesicles (80:20), whereas Span 40/Tween 40 forms spherical vesicles (50:50) and faceted vesicles (80:20) [8].

The number of acyl chains in Span 80 (one to four acyl chains) determines the curvature of vesicles [7]. Thus, the mixture ratio and chemical structure of Span and Tween affect the morphologies and surface properties of vesicles, which are related to their function [8–10].

Of the various morphologies of vesicles, the faceted vesicles have recently been brought to attention. The faceted vesicle is a polyhedral vesicle that contains membrane defects at the rim of the facets [11]. Such faceted vesicles can be formed from many different materials such as catanionic amphiphiles [12], block copolymers [13], phospholipids [11,14,15], and fatty acid/fluorinated fatty acid systems [16,17], rather than nonionic surfactants such as Span 40/Tween 40 [8]. For example, the mixture of fatty acid and fluorinated fatty acid can yield faceted vesicles by adjusting the pH of the fluorinated fatty acid [16,17]. Alternatively, a cooling of the temperature to below the phase-transition temperature results in a formation of gel-phase interdigitated membranes and a subsequent phase separation of a flexible rim and stiff facets to induce the faceted vesicles [11,18]. This phase separation has been revealed in the molecular dynamics study. Accordingly, the phase separation of Span 40 and Tween 40 might result in the formation of faceted vesicles although the details for mechanism have not been reported.

Conventionally, a hydration method is a well-known technique [9]. This method is usually combined with a freeze–thaw method to increase the size of the vesicles [1,2]. A two-step emulsification method was used to prepare vesicles made of the Span/Tween system [7–9]. However, these methods are batch-type, require complicated operations, and have the problem of using large amounts of organic solvents. Therefore, we recently reported a new preparation method that combines the subcritical water-assisted emulsification method (SCW) and the solvent diffusion method (DS), which is called the SCW/SD method [10]. Here, subcritical water is water that maintains its liquid state at high temperature and high pressure. A conceptual illustration of the SCW/SD is shown in Figure 1. First, a coarse O/W emulsion (size 800 nm) was produced by emulsifying a three-component water/oil/surfactant mixture. Thereafter, coarse O/W emulsions were mixed with the surfactant solution to a fine W/O/W emulsion (size 100 nm) by a hydrothermal treatment (240 °C and 10 MPa), which is the SCW step. Finally, the organic solvent was removed from the W/O/W emulsions to form vesicles (the SD step). Compared to conventional methods, the SCW/SD method enables continuous preparation, which simplifies the process and reduces the amount of organic solvent used [10]. This SCW/SD method can yield spherical vesicles made from the Span/Tween system [10]. However, the feasibility of preparing vesicles with other shapes is unknown. It is unclear whether faceted vesicles can be prepared. Hayashi et al. defined the angular vesicles obtained using Span 40/Tween 40 (80/20) as faceted vesicles. In addition, there have been no reports on their physical properties.
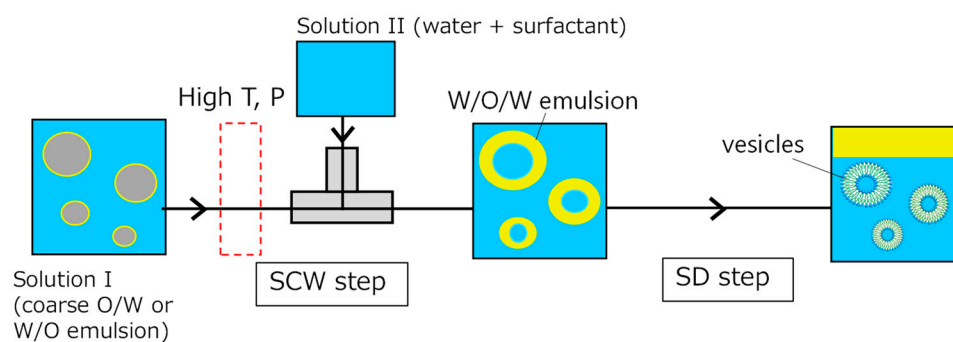

Figure 1. Conceptual illustration of SCW/SD method.

The major objective in this study was to demonstrate the possibility of preparing faceted vesicles using the SCW/SD method to characterize their membrane properties. For membrane properties, fluidity, hydrophobicity, and ζ-potential were studied, in accordance

with the reports [10,19]. In addition, the operating conditions for the preparation of faceted vesicles in this microcapillary system were discussed. These investigations would be helpful to understand the membrane properties of faceted vesicles made of Span 40/Tween 40 and their formation mechanism.

2. Materials and Methods

The Span 40 and Tween 40, decane, 1,6-diphenyl-1,3,5-hexatriene (DPH), Laurdan, and calcein were purchased from Wako Pure Chemical Co. Ltd. (Hiroshima, Japan). These chemical structures are shown in Figure 2.
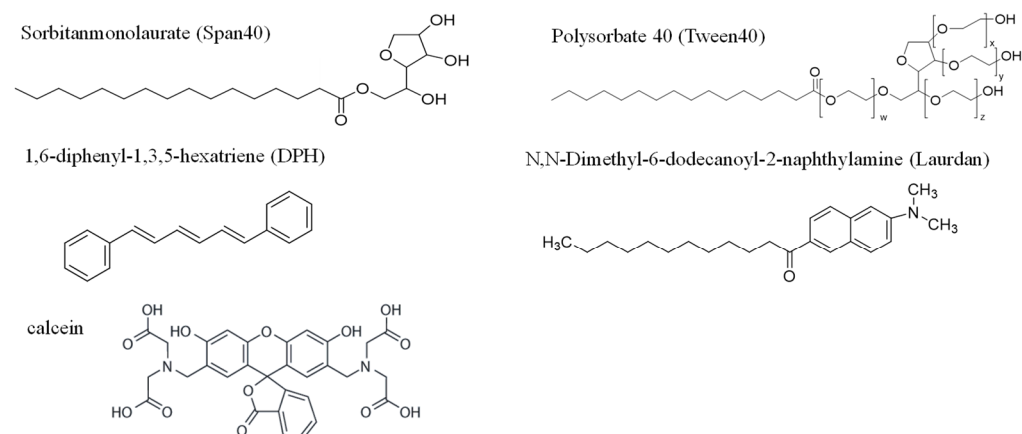
Figure 2. Chemical structures of surfactants and fluorescence probes.

2.1. SCW/SD Method

Decane was used as the organic phase and Span 40/Tween 40 was used as the surfactant. The mixture ratio of Span 40/Tween 40 altered from 50/50 to 100/0 wt/wt%. The three-component mixture was emulsified with a homogenizer (10,000 rpm, 3 min) to prepare a coarse emulsion, which was used as solution I. Solution I (0.3 m/min) was thereafter loaded into the microcapillary system under hydrothermal conditions (240 °C and 10 MPa), as shown in Figure 3. Afterwards, solution I was mixed with solution II (water + surfactants, 0.6 mL/min) using a T-junction. Notably, the flow rate of solution II to solution I reduced the amount of decane, which was advantageous for the removal of decane at the SD step. Thus, the subcritical water-assisted emulsification system allowed for the preparation of a W/O/W emulsion. The prepared W/O/W emulsion was kept for 24 or 48 h at 4 or 25 °C (SD step) to form the sample.
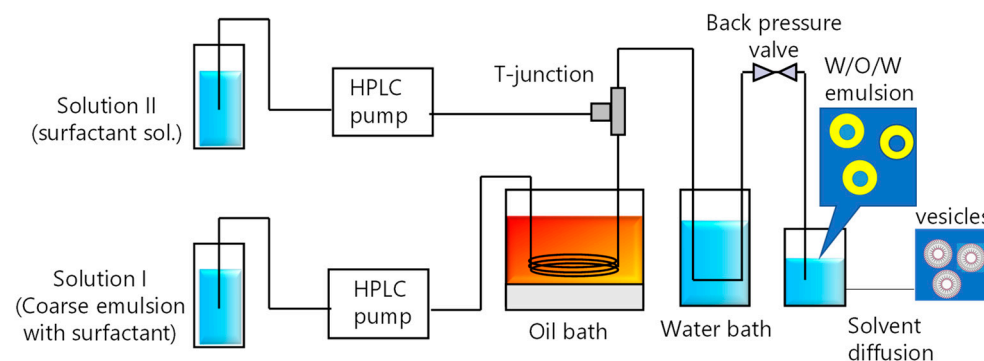
Figure 3. Schematic illustration of instruments used in this study.

2.2. Hydration Method

The conventional preparation method for faceted vesicles [8] was used for comparison with the SCW/SD method. First, a predetermined amount of surfactant was dissolved in

chloroform and poured into a round-bottom flask. Thereafter chloroform was evaporated using an evaporator to form a lipid thin film and dried overnight in a desiccator to completely remove the chloroform. The residual lipid thin film was hydrated with pure water, and the suspension was treated by the freeze–thaw method (5 times). Subsequently, the suspension was extruded using a polycarbonate filter with a pore size of 100 nm to adjust the vesicle size.

2.3. Membrane Characterization

Membrane properties such as size distribution, ζ-potential, membrane fluidity, and polar environment of the vesicle membranes were examined according to previous reports [8–10,19].

The size distribution of obtained samples was measured using a dynamic light scattering (DLS) technique, and the zeta potential was measured using a Zetasizer Nano ZS.

Membrane fluidity was evaluated based on the motility of the fluorescent probe DPH [8–11]. DPH was dissolved in ethanol at a concentration of 1 mM. An aliquot of the DPH–ethanol solution was mixed with the sample for 1 h at room temperature so that the sample could be considerably embedded with DPH. The final concentration ratio of lipid to DPH was 250:1. The sample was excited with vertically polarized light at 360 nm and the fluorescence intensities of parallel and perpendicular components, I_{pa} and I_{per}, respectively, were measured. The polarizability, P, of DPH was defined as follows:

$$P = (I_{pa} - I_{per})/(I_{pa} + I_{per}). \tag{1}$$

Membrane fluidity estimated using DPH was the reciprocal of P, $(1/P)_{DPH}$.

According to the literature [8], Laurdan's fluorescence properties are extremely sensitive to the polarity of the environment around the molecule itself. The emission spectrum exhibited a red shift owing to dielectric relaxation (Stokes shift). Laurdan was mixed with the sample at a lipid-to-laurdan molar ratio of 250:1. The general polarization (GP) was estimated from the emission spectra of Laurdan as follows:

$$GP_{340} = (I_{440} - I_{490})/(I_{440} + I_{490}) \tag{2}$$

where I_{440} and I_{490} are the fluorescence intensities at 440 and 490 nm, respectively. The GP_{340} value was obtained from the emission spectra using a shifted excitation wavelength of 340 nm. These measurements were performed in triplicates at 25 °C.

2.4. Calcein Leakage

The cobalt–calcein method was used according to a previous report [20]. Solution I, which contained calcein (1 mM) was loaded into the microcapillary system (see Figure 3). Faceted vesicles entrapping calcein were also obtained. Thereafter, $CoCl_2$ (100 mM) in excess of calcein was externally added to faceted vesicles to quench the calcein present at the outer aqueous phase of the vesicles. Faceted vesicles entrapping calcein were diluted by 100 times to initiate the calcein leakage experiment. The calcein fluorescence intensity was monitored by excitation and emission wavelengths of 490 and 520 nm, respectively. The released fraction of calcein (RF) was defined as follows:

$$RF\ [\%] = 100 \times (I_0 - I_t)/I_0 \tag{3}$$

where I_0 and I_t are the fluorescence intensity at time = 0 and t, respectively. This I_t value corresponds to the amount of calcein entrapped in the vesicles.

3. Results

3.1. Operational Conditions

3.1.1. Phase Diagram

It was previously reported that the lipid concentration of solution I is a key factor for the operational variable, which is related to the phase diagram of the ternary water/decane/surfactant system [10]. Figure 4a–c show the phase diagram of the ternary component systems obtained by changing the ratio of Span 40 to Tween 40. In the case of Span 40/Tween 40(50/50 *w/w*), a higher mixing ratio of surfactants could not be dissolved in the solvent (water/decane mixture), as shown in Figure 4a. With a decrease in the ratio of Tween 40 from 50 wt% to 0 wt%, the miscible region became narrower (Figure 4a–c). It should be noted that solution I in the immiscible region has the potential to cause a possible damage or clogging at the HPLC pump, T-junction, and back pressure valve. Therefore, the immiscible region was excluded from the possible operational conditions.
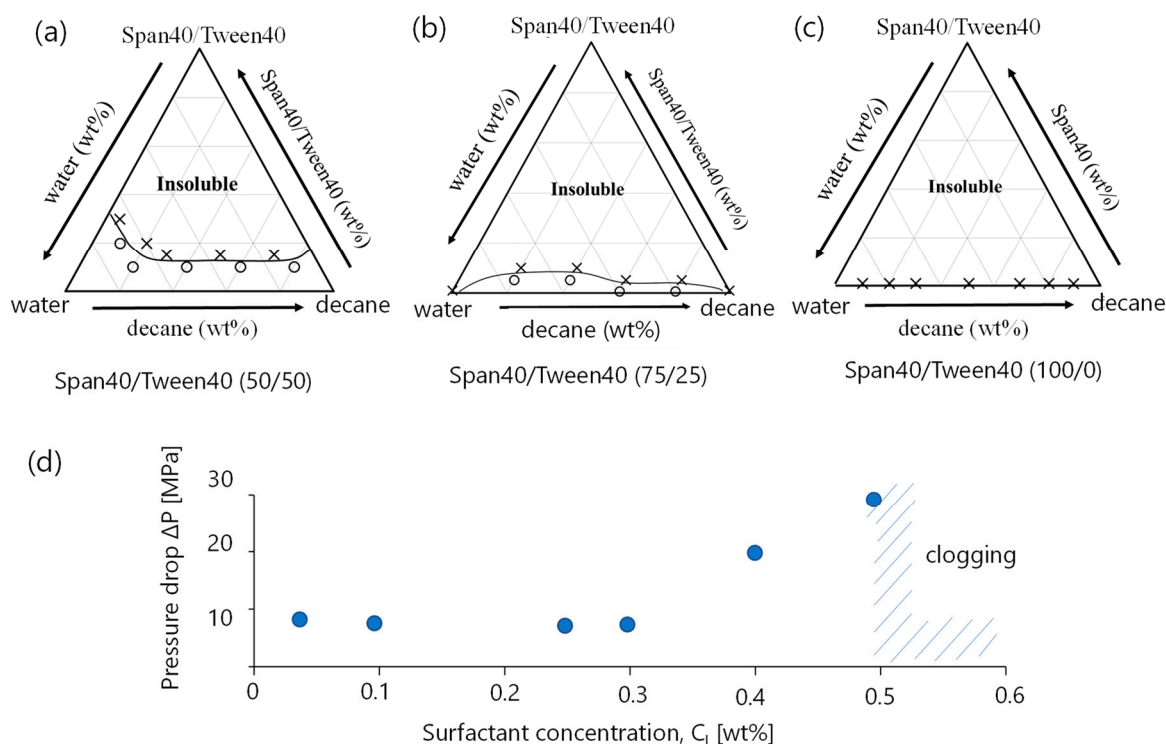

Figure 4. Phase diagram of ternary water/decane/surfactant systems of solution I (25 °C). (**a**) Span 40/Tween 40 (50/50), (**b**) Span 40/Tween 40 (75/25), and (**c**) Span 40/Tween 40 (100/0). (**d**) Concentration dependency of surfactant on pressure drop. Clogging occurred at the back pressure valve (see Figure 3). Symbols, ○ and ×, in (**a**–**c**) represent miscible and immiscible region, respectively.

3.1.2. Pressure Drop

According to the literature [8], faceted vesicles were obtained from Span 40/Tween 40 (75/25) to Span 40/Tween 40 (100/0). Thereby, Span 40/Tween 40 (80/20) was selected. Solution I at the lipid concentration of Span 40/Tween 40 was loaded into the microcapillary system, and the pressure drop at the HPLC pump was monitored. Figure 4d shows the relationship between the lipid concentration and pressure loss, DP. The DP value was maintained at approximately 10 MP below 0.3 wt% of surfactant. At above 0.3 wt%, the DP value increased. The DP value largely increased above 0.5 wt%, and solution I could not be loaded into the microcapillary. This was due to clogging at the back pressure valve, not at the pump and T-junction sites. Therefore, it was confirmed that the preparation of vesicles is difficult at lipid concentrations of 0.4 wt% or higher.

3.2. Formation Propensity of Vesicles

The samples obtained at lipid concentrations of 0.05 wt% and 0.25 wt% were observed using cryo-TEM. In the case of 0.05 wt%, emulsions were confirmed although whether they were spherical or faceted was not distinct. No vesicle was observed in the present tests (Figure 5a). The size distribution showed a single peak (Figure 5d). Therefore, the concentration of 0.05 wt% was unlikely to be advantageous for vesicle formation. In contrast, angular vesicles were observed at 0.25 wt% (Figure 5b,c). A cryo-TEM image of Type B vesicles is consistent with the observations previously reported [15–17,21–23]. The polydispersity indices (PDI) for Types A and B indicated 0.23–0.45 and 0.16–0.28, respectively. The solvent diffusion for 24 h favored a two-peak distribution rather than a single-peak distribution (Figure 5e). The first and second peaks were assigned to the lengths of minor and major axes in the faceted vesicles, respectively, which is called Type A. In the case of Figure 5c, a single peak was observed (Figure 5f). The faceted vesicle exhibited a morphology closer to angular and polyhedral than the lens-like vesicles reported previously [8]. Such a faceted vesicle, which is an angular vesicle, is called Type B.
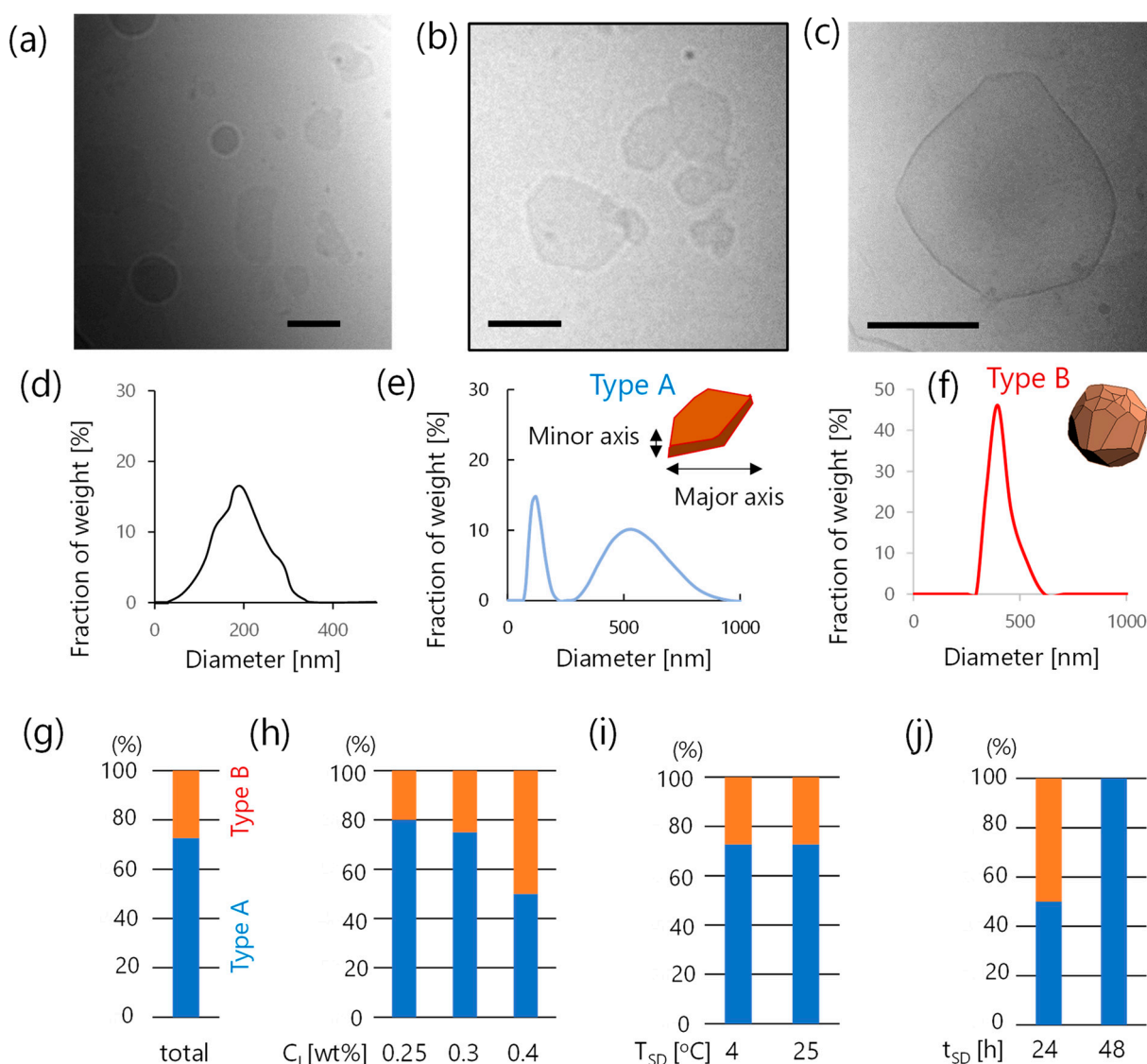

Figure 5. Representative cryo-TEM images and size distribution at (**a**,**d**) 0.05 wt%, (**b**,**e**) thin-faceted vesicles (Type A), (**c**,**f**) thick-faceted vesicles (Type B). Scale bar represents 100 nm in length. (**g**) Ratio of Types A and B (n = 22). Effect of (**h**) surfactant concentration of solution I, (**i**) temperature at SD, and (**j**) time of SD on ratio of Types A and B. Total number of trials was 22.

Next, we examined whether the operational variables determined Type A or B. All trials (n = 22) indicated mainly Type A as the major group (73%) as shown in Figure 5g. With a decrease in the surfactant concentration of solution I (C_I), Type A was favorably formed (Figure 5h). With respect to the influence of temperature at SD, no definite difference in the ratio of Types A and B was observed (Figure 5i). Therefore, the influence of time on SD was examined. The long SD time appeared to favor Type A (Figure 5j). Thus, the operational variables seem to influence vesicle formation to some extent.

3.3. Characterization of Faceted Vesicles

3.3.1. Membrane Properties

Based on the results of the previous section, the membrane properties of faceted vesicles were evaluated in terms of zeta potential, fluorescent probe motility, and the polar environment around the fluorescent probe [7–10,19].

Figure 6a shows the ζ-potential values of the samples obtained from the various preparation conditions for the SCW/SD method and the conventional method. The ζ-potential is the potential on the slipping surface, and the larger the ζ-potential value, the stronger the electrostatic repulsion between the particles and the higher the dispersibility [10]. The faceted vesicles prepared by the conventional method indicated the ζ-potential of -45.5 ± 5 mV. The ζ-potential of each sample prepared using the SCW/SD method was approximately -30 to -60 mV, regardless of the lipid concentration. Therefore, the obtained samples including the faceted vesicles, were considered highly dispersible and stable, regardless of the preparation method.
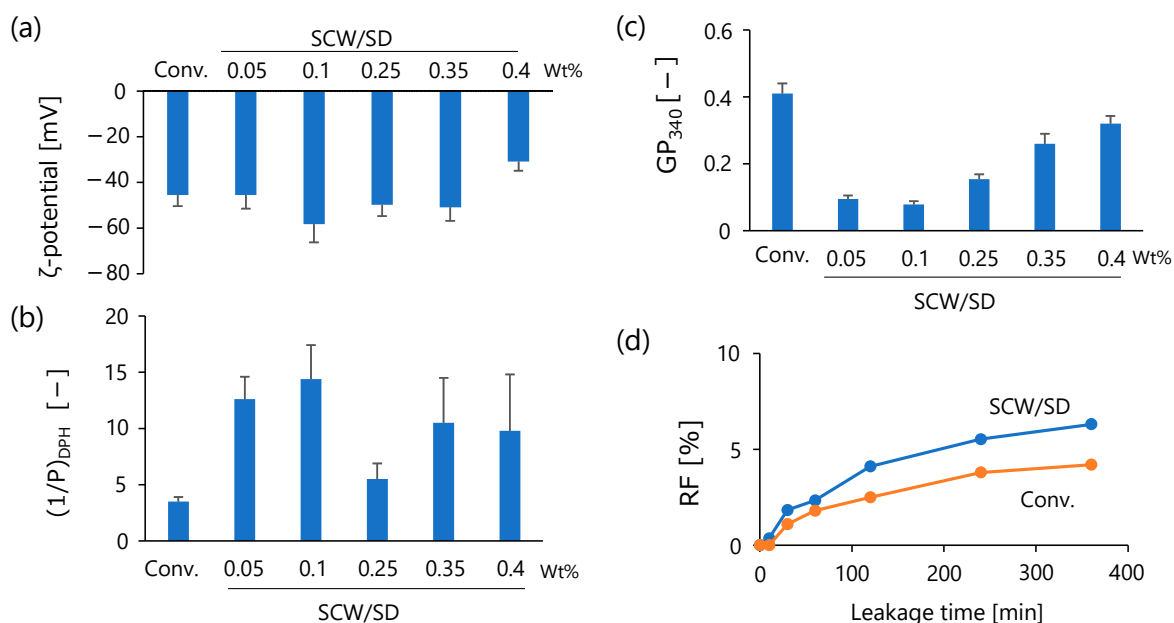

Figure 6. Comparison of various properties (**a**) ζ-potential, (**b**) mobility of DPH, and (**c**) generalized polarization of Laurdan. (**d**) Calcein leakage from faceted vesicle. (**d**) Calcein leakage behavior of vesicles prepared by the SCW/SD and conventional method. Conv.: conventional preparation method of faceted vesicles (see the Section 2.3). The error bar represents the standard error. All the experiments were at least triplicated.

Figure 6b shows membrane fluidity, which is the motility of the fluorescent probe DPH in the membrane. DPH motility was measured using the depolarization method. The higher the $(1/P)_{DPH}$ value (i.e., the higher the mobility of the DPH molecules), the higher the membrane fluidity. The faceted vesicles obtained by the conventional method indicated a $(1/P)_{DPH}$ value of 3.5 ± 0.4, which was lower than that of the spherical vesicles ($(1/P)_{DPH} \sim 10$ [10]). This strongly suggests that the faceted vesicles have rigid membranes. Span 40/Tween 40 (Span 40 80–100 wt%) was considered to be rigid at room temperature

owing to its phase transition temperature (40–50 °C) [8]. Next, the sample (0.25 wt%) had the lowest $(1/P)_{DPH}$ (6 to 7) of the samples prepared by the SCW/SD method, which was the closest value to the conventionally obtained faceted vesicles. The $(1/P)_{DPH}$ values 0.05 and 0.1 wt% were approximately 10–15, which corresponded to the observed emulsion.

Figure 6c shows the general polarization GP_{340} value for each sample obtained using Laurdan. The GP_{340} value is an index of the polar environment around the fluorescent probe, Laurdan. The larger the GP_{340} value, the more hydrophobic the surrounding environment. The conventionally prepared faceted vesicles had a GP_{340} value of 0.4 ± 0.03. This suggests that the membrane structure was hydrophobic. On the other hand, the GP_{340} values of samples prepared by the SCW/SD method (0.05–0.4 wt%) ranged from 0.1 to 0.3. Therefore, the membrane became more hydrophilic than the conventional faceted vesicles.

From the above results, the sample prepared with a lipid concentration of 0.25 wt% had the membrane properties closest to the conventionally prepared faceted vesicles.

3.3.2. Calcein Leakage Behavior

The encapsulation of calcein into faceted vesicles of Type A was examined to confirm the application of faceted vesicles as drug carriers. The faceted vesicles prepared at 0.25 wt% indicated the Type A vesicles from the size distribution measurement (Figure 5e,h). Additionally, the treatment of the vesicle suspension with Triton X-100 resulted in zero fluorescence intensity, suggesting the successful entrapment of calcein. Next, Figure 6d shows the time–course of the RF value. The RF value was 6.3% after 360 min. In addition, the RF value of the present samples indicated a higher RF value for conventionally prepared faceted vesicles. It is possible that the residual decane in the vesicle membranes perturbed the membrane structure to increase the permeability to calcein. Considering that the RF value of spherical vesicles is approximately 3–4%, faceted vesicles are capable of encapsulating calcein.

4. Discussion

The present preparation method resulted in the formation of vesicles or emulsions (Figure 5a–c). This propensity to form might depend on the state of the coarse emulsion. Generally, the homogenization of water/decane/surfactant mixtures at a high water content might favor a coarse O/W emulsion. After hydrothermal emulsification, O/W emulsions 100 nm in size were produced, as shown in Figure 5a. This was because (1) the amount of surfactant covering the surface of the W/O/W emulsions was insufficient, or (2) because the water content of solution I was too high to form an O/W emulsion rather than a W/O emulsion. The latter case might be that a reduced-size O/W emulsion obtained via hydrothermal treatment. Therefore, the successful formation of vesicles would require an adequate water-to-decane volume ratio and a sufficient concentration of surfactants.

Whether a mixture of Span 40/Tween 40 (80/20) possesses the ability to form the faceted shape in the SCW/SD method is herein discussed. The W/O/W emulsion before the SD step indicated that there were not definite faceted emulsion droplets (e.g., Figure 5a). It was considered that Span 40 and Tween 40 might be insufficient for covering W/O/W emulsions. Previously, faceted O/W emulsion droplets made of cationic surfactant, octadecyltrimethylammonium bromide plus salt were stable, owing to the formation of a frozen interfacial layer at the oil–water interface [24]. It is, therefore, considered that Span 40/Tween 40 can form the stiff interface-like frozen interfacial layer because of the phase–transition temperature: Span 40 (40–50 °C) and Tween 40 (<10 °C) [8]. Figure 5a shows that it was unclear whether O/W emulsion droplets had a faceted shape. This might result from insufficient concentration of Span 40 and Tween 40 for a coverage of emulsions after a SD step. In the SD step, lateral diffusion of surfactants was altered in the process of the diffusion of decane from W/O/W emulsions. From the observations of faceted vesicles (Figure 5b,c), the pair of curvatures were produced, accompanied with the phase separation between Span 40 and Tween 40. According to the literature [8], this process originated from the difference between their headgroup structures (see Figure 2). Berton et al. have

reported that the lateral heterogeneity in the interface of O/W emulsions resulted from the different structures of surfactants [25], which supports the possible mechanism mentioned above. Thus, a mixture of Span 40/Tween 40 (80/20) led to the shape of faceted in the SCW/SD method.

In the latter period of the SD step, the rims should occur at the surface of the vesicles. Tween 40 might be localized, especially at the rims, owing to a phase separation which resulted from a difference in headgroup structure between Span 40 (cylinder type, $a_0 = 0.37$ nm^2) and Tween 40 (cone type, $a_0 = 0.533$ nm^2) [26]. This mechanism is similar to the mechanism that cationic surfactants with large headgroups locate at the outer rims and anionic surfactants with smaller headgroups locate at the inner rims by flip-flop [27]. However, such a heterogeneity of Tween 40 could not be detected from the cryo-TEM observations (e.g., Figure 5b,c) because oligoethylene glycol, that is the hydrophilic head of Tween 40, could not be observed by cryo-TEM. This is because there is no significant difference in electron density compared to water [10,28]. For this reason, another scenario is also noted: that a formation of faceted vesicles is a result of the difference in lipids between the outer and inner leaflet of a gel-phase interdigitated membranes [11,18]. Next, the facets seemed to consist of Span 40, and were at a gel state because of its phase-transition temperature (40–50 °C) being greater than the SD temperature (4 °C or 25 °C) [8]. A conventional formation mechanism of spherical vesicles results from the bending induced in the lamellar structure with open ends (a flake-like membrane [29,30] or bicell [31–33]). It was clarified that this curvature correlated with the $(1/P)_{DPH}$ value from the studies using giant vesicles [34,35]. Therefore, the membrane of the Span 40-rich region with low $(1/P)_{DPH}$ (Figure 6b) could not be bent, which is consistent with the observation (Figure 5b,c). Thus, the facets formed by Span 40 and the rim formation by Tween 40 led to the faceted vesicles. In other words, it could be concluded that the SCW/SD method gave the faceted vesicles of Span 40/Tween 40 (80/20).

As shown in Figure 5, the faceted vesicles contained Types A and B. Why Type A rather than Type B vesicles were more likely to be formed is discussed. Type B vesicles have more rims than Type A vesicles (see Figure 5e,f). Type A vesicles, having major and minor axes, possess the side with large curvature corresponding to the minor axis. Tween 40 could then be gathered at the side, which is advantageous for Tween 40 which has a large headgroup relative to Span 40. In contrast, Type B vesicles required more rims than Type A vesicles. This would be entropically unfavorable if Tween 40 molecules gathered at the side of Type A vesicles and were reorientated into new rims on Type B vesicles (i.e., the transition of Type A to Type B vesicles), although the energetical study should be examined. However, it has been shown that faceted structures can be low energy configurations of elastic spherical vesicles [23,36–38]. If so, the faceted vesicles closer to the spherical vesicle (Type B) might be more stable than Type A vesicles. This might result from the larger and more steric headgroup of Tween 40 than other surfactants such as catanionic amphiphiles [12], diamidophospholipids [11,14], and fatty acid/fluorinated fatty acid systems [16,17]. As long as the Span 40/Tween 40 system is nonionic, it is, therefore, considered that Type A rather than Type B vesicles were observed in the present experiment.

Finally, we discuss why the calcein leakage occurred at the gel state (Figure 6d). Generally, the lipid membranes at a gel state indicate there is low permeability to calcein [39–41]. It is therefore the bent region, rather than Span 40-rich planes at the gel state, that is responsible for calcein leakage. This is related to the restriction of a free volume in lipid membranes [41] and to an ordered structure of acyl chain at the gel state [42]. The bending of vesicle membrane associated with the localization of Tween 40 would increase the free volume and reduce the ordered structure of the acyl chain. In addition, vesicles made of Span 40 (GP$_{340}$ = 0.6 ± 0.04) indicated a higher GP$_{340}$ value than Span 40/Tween 40 (80/20 wt/wt%) (GP$_{340}$ = 0.1–0.2, see Figure 6c), which is in agreement with the previous report [8]. This suggests that the rim (Tween 40) is more hydrophilic than the facets

(Span 40-rich region). From this viewpoint, it could be considered that calcein favored the leakage via the rims where Tween 40 was located.

5. Conclusions

In this study, we investigated if the SCW/SD method could be used to prepare faceted vesicles. From the phase diagram study, Span 40/Tween 40 (80/20 wt%/wt%) was selected as a possible condition to prepare solution I. Faceted vesicles were obtained in the lipid concentration range of 0.2 to 0.3 wt%. However, an emulsion was observed at 0.05–0.1 wt%. On the other hand, the clogging phenomena occurred at wt% above 0.4, inhibiting the vesicle formation. Next, membrane properties of faceted vesicles obtained were evaluated in terms of size distribution, ζ-potential, membrane fluidity, and polarity. As a result, it was found that faceted vesicles with short and long axes (Type A) are easier to form than angular vesicles close to spherical vesicles (Type B). The formation propensity of both types seemed to depend on the lipid concentration, the temperature, or the time of the SD step. In addition, the ζ potential showed a large negative value, suggesting the dispersibility of the faceted vesicles. Their membrane fluidity was found to be lower than that of spherical vesicles, suggesting that the membrane is rigid. The polarity measurement using Laurdan suggested there was a hydrophobic membrane environment. Therefore, it was expected that the angular region (edges and vertices) of the faceted vesicles was generated by an orientation of Tween 40 with phase separation, preventing the interior of the lipid membrane from being exposed to the bulk aqueous phase. Such faceted vesicles of Type A are expected to serve as alternative carriers for bicelles with a low encapsulation efficiency for drugs.

Author Contributions: Conceptualization, T.S.; methodology, T.S.; formal analysis, Y.K. (Yui Komori); investigation, Y.K. (Yui Komori) and K.T.; data curation, Y.K. (Yukitaka Kimura); writing—original draft preparation, T.S.; writing—review and editing, T.S., K.H., K.Y., H.-S.J. and Y.K. (Yukitaka Kimura); supervision, T.S. and Y.K. (Yukitaka Kimura); funding acquisition, T.S. and H.-S.J. All authors have read and agreed to the published version of the manuscript.

Institutional Review Board Statement: Not applicable.

Informed Consent Statement: Not applicable.

Data Availability Statement: Not applicable.

Conflicts of Interest: The authors declare no conflict of interest.

References

1. Guimarães, D.; Cavaco-Paulo, A.; Nogueira, E. Design of liposomes as drug delivery system for therapeutic applications. *Int. J. Pharm.* **2021**, *601*, 120571. [CrossRef] [PubMed]
2. Walde, P.; Cosentino, K.; Engel, H.; Stano, P. Giant vesicles: Preparations and applications. *ChemBioChem* **2010**, *11*, 848–865. [CrossRef] [PubMed]
3. Tenchov, R.; Bird, R.; Curtze, A.; Zhou, Q. Lipid Nanoparticles–From Liposomes to mRNA Vaccine Delivery, a Landscape of Research Diversity and Advancement. *ACS Nano* **2021**, *15*, 16982–17015. [CrossRef] [PubMed]
4. Ge, X.; Wei, M.; He, S.; Yuan, W.-E. Advances of Non-Ionic Surfactant Vesicles (Niosomes) and Their Application in Drug Delivery. *Pharmaceutics* **2019**, *11*, 55. [CrossRef]
5. Chen, S.; Hanning, S.; Falconer, J.; Locke, M.; Wen, J. Recent advances in non-ionic surfactant vesicles (niosomes): Fabrication, characterization, pharmaceutical and cosmetic applications. *Eur. J. Pharm. Biopharm.* **2019**, *144*, 18–39. [CrossRef]
6. Araste, F.; Aliabadi, A.; Abnous, K.; Taghdisi, S.M.; Ramezani, M.; Alibolandi, M. Self-assembled polymeric vesicles: Focus on polymersomes in cancer treatment. *J. Control. Release* **2021**, *330*, 502–528. [CrossRef]

7. Kato, K.; Walde, P.; Koine, N.; Ichikawa, S.; Ishikawa, T.; Nagahama, R.; Ishihara, T.; Tsujii, T.; Shudou, M.; Omokawa, Y.; et al. Temperature-Sensitive Nonionic Vesicles Prepared from Span 80 (Sorbitan Monooleate). *Langmuir* **2008**, *24*, 10762–10770. [CrossRef]

8. Hayashi, K.; Iwai, H.; Kamei, T.; Iwamoto, K.; Shimanouchi, T.; Fujita, S.; Nakamura, H.; Umakoshi, H. Tailor-made drug carrier: Comparison of formation-dependent physicochemical properties within self-assembled aggregates for an optimal drug carrier. *Colloids Surf. B Biointerfaces* **2017**, *152*, 269–276. [CrossRef]

9. Hayashi, K.; Shimanouchi, T.; Kato, K.; Miyazaki, T.; Nakamura, A.; Umakoshi, H. Span 80 vesicles have a more fluid, flexible and "wet" surface than phospholipid liposomes. *Colloids Surf. B Biointerfaces* **2011**, *87*, 28–35. [CrossRef]

10. Shimanouchi, T.; Hayashi, T.; Toramoto, K.; Fukuma, S.; Hayashi, K.; Yasuhara, K.; Kimura, Y. Microfluidic and hydrothermal preparation of vesicles using sorbitan monolaurate/polyoxyethylene (20) sorbitan monolaurate(Span20/Tween20). *Colloids Surf. B Biointerfaces* **2021**, *205*, 111836. [CrossRef]

11. Zumbuehl, A. Artificial Phospholipids and Their Vesicles. *Langmuir* **2018**, *35*, 10223–10232. [CrossRef] [PubMed]

12. Dubois, M.; Demé, B.; Gulik-Krzywicki, T.; Dedieu, J.-C.; Vautrin, C.; Désert, S.; Perez, E.; Zemb, T. Self-assembly of regular hollow icosahedra in salt-free catanionic solutions. *Nature* **2001**, *411*, 672–675. [CrossRef]

13. Deng, Y.; Ling, J.; Li, M. Physical stimuli-responsive liposomes and polymersomes as drug delivery vehciles based on phase transitions in the membrane. *Nanoscale* **2018**, *10*, 6781–6800. [CrossRef]

14. Rosa, M.; Infante, M.R.; Miguel, M.d.G.; Lindman, B. Spontaneous Formation of Vesicles and Dispersed Cubic and Hexagonal Particles in Amino Acid-Based Catanionic Surfactant Systems. *Langmuir* **2006**, *22*, 5588–5596. [CrossRef]

15. Feitosa, E. Spontaneous vesicles of sodium dihexadecylphosphate in HEPES buffer. *J. Colloid Interface Sci.* **2008**, *320*, 608–610. [CrossRef]

16. González-Pérez, A.; Schmutz, M.; Waton, G.; Romero, M.J.; Krafft, M.P. Isolated Fluid Polyhedral Vesicles. *J. Am. Chem. Soc.* **2007**, *129*, 756–757. [CrossRef]

17. Zhang, J.; Xu, G.; Song, A.; Wang, L.; Lin, M.; Dong, Z.; Yang, Z. Faceted fatty acid vesicles formed from single-tailed perfluorinated surfactants. *Soft Matter* **2015**, *11*, 7143–7150. [CrossRef]

18. Noguchi, H. Polyhedral vesicles: A Brownian dynamics simulation. *Phys. Rev. E* **2003**, *67*, 041901. [CrossRef]

19. Bui, T.T.; Suga, K.; Umakoshi, H. Roles of Sterol Derivatives in Regulating the Properties of Phospholipid Bilayer Systems. *Langmuir* **2016**, *32*, 6176–6184. [CrossRef]

20. Shimanouchi, T.; Kawasak, H.; Fuse, M.; Umakoshi, H.; Kuboi, R. Membrane fusion mediated by phospholipase C under endo-somal pH conditions. *Coll. Surf. B* **2013**, *103*, 75–83. [CrossRef]

21. Tribet, C.; Vial, F. Flexible macromolecules attached to lipid bilayers: Impact on fluidity, curvature, permeability and stability of the membranes. *Soft Matter* **2007**, *4*, 68–81. [CrossRef] [PubMed]

22. Castangia, I.; Manca, M.L.; Caddeo, C.; Maxia, A.; Murgia, S.; Pons, R.; Demurtas, D.; Pando, D.; Falconieri, D.; Peris, J.E.; et al. Faceted phospholipid vesicles tailored for the delivery of Santolina insularis essential oil to the skin. *Colloids Surf. B Biointerfaces* **2015**, *132*, 185–193. [CrossRef] [PubMed]

23. Shen, Y.; Ou-Yang, Z.-C.; Hao, J.; Lin, H.; Jiang, L.; Liu, Z.; Gao, X. The mechanism for the transition from vesicles to punctured lamellae and faceted vesicles in cationic and anionic fluorinated surfactant mixture. *Colloids Surf. A Physicochem. Eng. Asp.* **2016**, *500*, 40–44. [CrossRef]

24. Nanikashvili, P.M.; Butenko, A.V.; Deutsch, M.; Lee, D.; Sloutskin, E. Salt-induced stability and modified interfacial energetics in self-faceting emulsion droplets. *J. Colloid Interface Sci.* **2022**, *621*, 131–138. [CrossRef] [PubMed]

25. Berton, C.; Genot, C.; Guibert, D.; Ropers, M.-H. Effect of lateral heterogeneity in mixed surfactant-stabilized interfaces on the oxidation of unsaturated lipids in oil-in-water emulsions. *J. Colloid Interface Sci.* **2012**, *377*, 244–250. [CrossRef]

26. Hayashi, K.; Iwai, H.; Shimanouchi, T.; Umakoshi, H.; Iwasaki, T.; Kato, A.; Nakamura, H. Formation of lens-like vesicles induced via microphase separations on a sorbitan monoester membrane with different headgroups. *Colloids Surf. B Biointerfaces* **2015**, *135*, 235–242. [CrossRef]

27. Chen, Y.; Qiao, F.; Fan, Y.; Han, Y.; Wang, Y. Interactions of Phospholipid Vesicles with Cationic and Anionic Oligomeric Surfactants. *J. Phys. Chem. B* **2017**, *121*, 7122–7132. [CrossRef]

28. Kunstsche, J.; Horst, J.; Bunjes, H. Cryogenic transimission electron microscopy (cryo-TEM) for studying the morphology of colloidal drug delivery systems. *Int. J. Pharm.* **2011**, *417*, 120–137. [CrossRef]

29. Lasic, D.D. Mechanisms of Liposome Formation. *J. Liposome Res.* **1995**, *5*, 431–441. [CrossRef]

30. Zook, J.M.; Vreeland, W.N. Effects of temperature, acyl chain length, and flow-rate ratio on liposome formation and size in a microfluidic hydrodynamic focusing device. *Soft Matter* **2010**, *6*, 1352–1360. [CrossRef]

31. Sanders, C.R.; Landis, G.C. Reconstitution of Membrane Proteins into Lipid-Rich Bilayered Mixed Micelles for NMR Studies. *Biochemistry* **1995**, *34*, 4030–4040. [CrossRef]

32. Vold, R.R.; Prosser, R. Magnetically Oriented Phospholipid Bilayered Micelles for Structural Studies of Polypeptides. Does Ideal Bicelle Exist? *J. Magn. Reson. Ser. B* **1996**, *113*, 267–271. [CrossRef]

33. Dugourc, E. Bicelles and nanodiscs for biophysical chemistry. *Biochim. Biophys. Acta-Biomembr.* **2021**, *1863*, 183478. [CrossRef]

34. Shimanouchi, T.; Umakoshi, H.; Kuboi, R. Kinetic Study on Giant Vesicle Formation with Electroformation Method. *Langmuir* **2009**, *25*, 4835–4840. [CrossRef]

35. Shimanouchi, T.; Umakoshi, H.; Kuboi, R. Growth behavior of giant vesicles using the electroformation method: Effect of proteins on swelling and deformation. *J. Colloid Interface Sci.* **2013**, *394*, 269–276. [CrossRef]
36. Bowick, M.J.; Sknepnek, R. Pathways to faceting of vesicles. *Soft Matter* **2013**, *9*, 8088–8095. [CrossRef]
37. Olvera de la Cruz, M. Mesoscale studies of ionic closed membranes with polyhedral geometries. *APL Mater.* **2016**, *4*, 061102. [CrossRef]
38. Guttman, S.; Ocko, B.M.; Deutsch, M.; Sloutskin, E. From faceted vesicles to liquid icoshedra: Where topology and crystallography meet. *Curr. Opin. Colloid Interface Sci.* **2016**, *22*, 35–40. [CrossRef]
39. Shimanouchi, T.; Ishii, H.; Yoshimoto, N.; Umakoshi, H.; Kuboi, R. Calcein permeation across phosphatidylcholine bilayer membrane: Effects of membrane fluidity, liposome size, and immobilization. *Colloids Surf. B Biointerfaces* **2009**, *73*, 156–160. [CrossRef]
40. Fukuma, S.; Shimanouchi, T.; Hayashi, K.; Kimura, Y. Calcein Leakage Behavior from Vesicles Induced by Protein–Vesicle Interaction: A Study by Surface Pressure–Area Isotherms. *Chem. Lett.* **2017**, *46*, 1036–1039. [CrossRef]
41. Maherani, B.; Arab-Tehrany, E.; Kheirolomoom, A.; Geny, D.; Linder, M. Calcein release behavior from liposomal bilayer; influ-ence of physicochemical/mechanical/structural properties of lipids. *Biochimie* **2013**, *95*, 2018–2033. [CrossRef] [PubMed]
42. Xiang, T.-X.; Anderson, B.D. Influence of Chain Ordering on the Selectivity of Dipalmitoylphosphatidylcholine Bilayer Membranes for Permeant Size and Shape. *Biophys. J.* **1998**, *75*, 2658–2671. [CrossRef] [PubMed]